



Hardware Article



Low cost, portable, 3D printable tissue precision slicer

Beatriz Martinez-Martin ^a, Isabella Lambros ^b, Lukas Nuesslein ^b, Yubing Sun ^{a,b,c,*}^a Molecular and Cellular Biology Graduate Program, University of Massachusetts Amherst, Amherst, MA 01003, United States^b Department of Mechanical and Industrial Engineering, University of Massachusetts Amherst, Amherst, MA 01003, United States^c Department of Biomedical Engineering, University of Massachusetts Amherst, Amherst, MA 01003, United States

ARTICLE INFO

Keywords:

Tissue slices
Microtomy
Organoids
Low-cost

ABSTRACT

Slicing tissue samples into thin pieces is commonly used in histology analysis and more recently for organotypic culture when tissue samples are sliced alive. Currently available devices for slicing tissue samples are either designed for fixed tissue samples at low cryogenic temperatures (e.g., Cryostats), or bulky and expensive (e.g., vibratome), preventing them from routine lab usage. Here we report a cost-effective device designed to section live tissues for subsequent culture. This device consists of components crafted from 3D-printed Nylon-12- a material suitable for autoclaving to ensure sterility. Its small footprint enhances portability, allowing for convenient placement within a biosafety cabinet for an added layer of sterility assurance. Using human pluripotent stem cells derived brain organoids as an example, we demonstrated that the device both precisely and accurately makes slices. We further validate its suitability for long-term culture by extended tissue culture following slicing. Our results indicate that brain organoid slices are viable and show improved proliferation rate compared with unsliced organoids.

1. Specifications table

| | |
|---------------------------|--|
| Hardware name | Live Tissue Precision Slicer |
| Subject area | <ul style="list-style-type: none"> Engineering and materials science Neuroscience Biological sciences Imaging tools Biological sample handling and preparation Mechanical engineering and materials science Vibratome Cryostat |
| Hardware type | CC-BY-NC 4.0 |
| Closest commercial analog | ~\$853.21 USD |
| Open source license | https://doi.org/10.17632/p3npz8wkny.2 |
| Cost of hardware | |
| Source file repository | |

* Corresponding author at: Molecular and Cellular Biology Graduate Program, University of Massachusetts Amherst, Amherst, MA 01003, United States.

E-mail address: ybsun@umass.edu (Y. Sun).

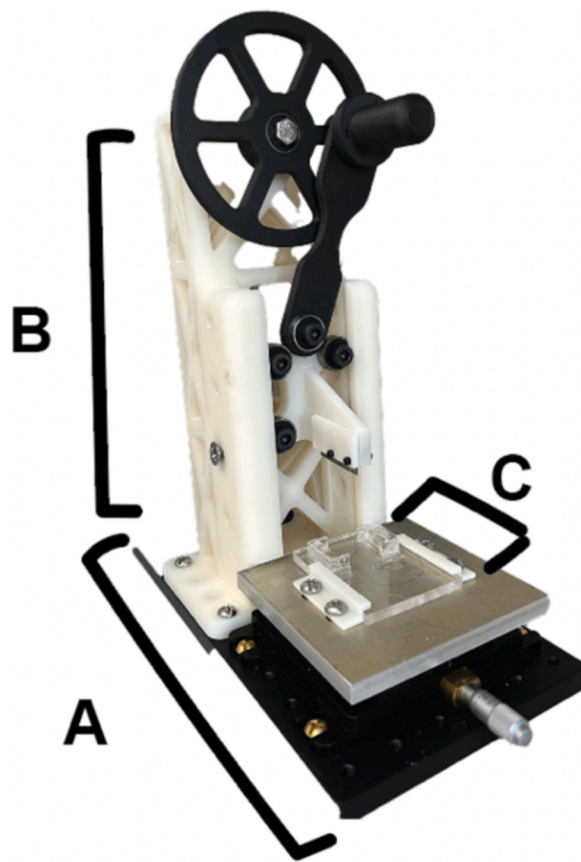


Fig. 1. A photograph of the live tissue precision slicer. The device is mainly composed of a base with a motion plate (A), an arm with cutting blades (B), and a box (C) to hold agarose gel embedded tissues.

2. Hardware in context

Tissue slicing is a widely employed technique in laboratories for diverse applications such as immunohistochemistry, electrophysiological analysis, *in situ* hybridization, and electron microscopy [1–3]. Recently, this method has been employed in the realm of live tissues such as organoids. Slicing organoids addresses the diffusion limits of nutrient and oxygen, and thus enables extended culture for improved viability and functional maturation [4]. For brain organoids, the sliced organoids have improved adhesion to planar multielectrode arrays, making it ideal for electrophysiological assessments [5]. Researchers typically utilize a microtome within a cryostat to section fixed tissue samples. However, this traditional approach relies on a biocompatible adhesive that solidifies only at extremely low temperatures, rendering it unsuitable for live tissue samples.

Considering the vulnerability of living tissues to such low temperatures, an alternative cutting method becomes imperative. Vibrating microtomes, or vibratomes, offer a solution for slicing live tissue [1]; however, they can be prohibitively expensive. On the more cost-effective and basic side, vibratomes are available from \$5,000–\$15,000 USD and more advanced models with additional features range from \$20,000–\$50,000 USD. Typical vibratome systems occupy significant spaces in a biosafety cabinet (BSC), and it is inconvenient to thoroughly sterilize the equipment given the complex geometry and delicate electrical components. Thus, a simple, cost-effective, and robust slicer is needed particularly for live-tissue slice culture.

This hardware was developed with three primary objectives: 1) **Cost effectiveness:** Providing an economical option for tissue slicing applicable to both live and fixed tissues; 2) **Optimization for live tissue:** Featuring a small form factor for compatibility with a BSC and standard sterilization practices; 3) **Precision and consistency:** reaching an accuracy of 0.25 μm for slice thickness without sacrificing cell viability. In this innovative design, organoids are suspended in agarose and secured within a biocompatible acrylic box, eliminating the need for the repeated purchase of adhesive material as the box is reusable. Here we demonstrate the feasibility of using this device for cutting live brain organoids. With some modifications, this device can be applied broadly for slicing multiple types of live or fixed tissues.

3. Hardware description

In its simplest form, this equipment is a highly precision slicing machine specifically designed to slice live tissue although it can be

adapted for slicing fixed samples as well. The hardware comprises fundamental screws and bearings readily available at a hardware store or through online machining vendors. The machine is structured around three key components: the base, the arm, and the box (Fig. 1). The machine's base functions as a motion stage, allowing for adjustments to achieve various cut sizes. The machine's arm is constructed from 3D printed Nylon-12 pieces that seamlessly interlock with screws and bearings, facilitating an intuitive and swift assembly process using only wrenches and screwdrivers. The machine's box is composed of acrylic, and this is where the sample will be mounted to slice while embedded in agarose. Operating as a fully manual system, this machine enables easy customization of cuts, as well as overall hardware adjustments and optimizations tailored to your specific processes. Compared to a vibratome or a cryostat, this machine is significantly more cost effective and allows for live tissue slicing followed by long-term culturing. While varying by brand, vibratomes typically weigh around 15 kg, and cryostats weigh approximately 193 kg. In comparison, our machine weighs 7 kg, making it significantly smaller and more portable. The time required to section an entire organoid depends on its size and the desired slice thickness. For instance, once mounted, slicing at 300 μ m using a vibratome takes approximately 30 min, and a cryostat takes approximately 20 min, whereas our device only requires about 1 min per slice. Our slicer offers a range of slice thicknesses from 250 μ m to 1 mm, providing a comparable resolution to commercially available devices. Our data show that this slicer robustly makes quick and precise cuts to small tissue samples (less than 1 mm) with easily adjustable cut size.

Design files.

4. Design files summary

| Design file name | File type | Open source license | Location of the file |
|------------------------------|-----------|---------------------|---|
| Acrylic_Box.SLDASM | CAD file | CC-BY-NC 4.0 | https://doi.org/10.17632/p3npz8wkny.2 |
| Acrylic_Box_and_Shell.SLDASM | CAD file | CC-BY-NC 4.0 | https://doi.org/10.17632/p3npz8wkny.2 |
| Acrylic_Shell.SLDASM | CAD file | CC-BY-NC 4.0 | https://doi.org/10.17632/p3npz8wkny.2 |
| Arm_Base.SLDPRT | CAD file | CC-BY-NC 4.0 | https://doi.org/10.17632/p3npz8wkny.2 |
| Crank.SLDPRT | CAD file | CC-BY-NC 4.0 | https://doi.org/10.17632/p3npz8wkny.2 |
| Large_Insert.SLDPRT | CAD file | CC-BY-NC 4.0 | https://doi.org/10.17632/p3npz8wkny.2 |
| Lever.SLDPRT | CAD file | CC-BY-NC 4.0 | https://doi.org/10.17632/p3npz8wkny.2 |
| Pin_Wall.SLDPRT | CAD file | CC-BY-NC 4.0 | https://doi.org/10.17632/p3npz8wkny.2 |
| Precision_Slicer.SLDASM | CAD file | CC-BY-NC 4.0 | https://doi.org/10.17632/p3npz8wkny.2 |
| Razor_Fastener.SLDPRT | CAD file | CC-BY-NC 4.0 | https://doi.org/10.17632/p3npz8wkny.2 |
| Razor_Holder.SLDPRT | CAD file | CC-BY-NC 4.0 | https://doi.org/10.17632/p3npz8wkny.2 |
| Razor_Holder_Assembly.SLDASM | CAD file | CC-BY-NC 4.0 | https://doi.org/10.17632/p3npz8wkny.2 |
| Shelf.SLDPRT | CAD file | CC-BY-NC 4.0 | https://doi.org/10.17632/p3npz8wkny.2 |
| Slotted_Wall.SLDPRT | CAD file | CC-BY-NC 4.0 | https://doi.org/10.17632/p3npz8wkny.2 |
| Small_Insert.SLDPRT | CAD file | CC-BY-NC 4.0 | https://doi.org/10.17632/p3npz8wkny.2 |
| Wheel.SLDPRT | CAD file | CC-BY-NC 4.0 | https://doi.org/10.17632/p3npz8wkny.2 |

5. Bill of materials summary

| Component | Number | Cost per unit- USD | Total cost- USD | Source of materials | Material type |
|---|-----------------------------|-----------------------|--------------------|---|------------------|
| M8x1.25 Mm nut | pkg. 100 | \$9.67 | \$9.67 | https://mcmaster.com | Steel |
| M8x1.25 Mm thread, 150 Mm long bolt | pkg. 5 | \$9.52 | \$9.52 | https://mcmaster.com | Steel |
| M8x1.25 Mm thread, 130 Mm long bolt | 1 | \$3.50 | \$3.50 | https://mcmaster.com | Steel |
| M8x1Mm thread, 30 Mm long bolt | pkg. 5 | \$9.20 | \$9.20 | https://mcmaster.com | Alloy Steel |
| M2.5x0.45 Mm thread nut | pkg. 100 | \$4.19 | \$4.19 | https://mcmaster.com | Alloy Steel |
| M2.5x 0.45 Mm thread, 15 Mm long bolt | pkg. 5 | \$16.82 | \$16.82 | https://mcmaster.com | Alloy Steel |
| M2.5x0.45 Mm thread, 10 Mm long bolt | pkg. 100 | \$6.54 | \$6.54 | https://mcmaster.com | Steel |
| M6x1Mm thread, 10 Mm long bolt | pkg. 100 | \$14.57 | \$14.57 | https://mcmaster.com | Alloy Steel |
| M7x1Mm thread, 10 Mm long bolt | pkg. 25 | \$6.07 | \$6.07 | https://mcmaster.com | Steel |
| 8x22x7mm rolling bearing | pkg. 100 | \$18.79 | \$18.79 | https://amazon.com | Steel |
| ¼" Acrylic sheet | 1 | \$24.09 | \$24.09 | https://interstateplastics.com | Acrylic |
| Two-axis linear translation stage with rotating platform | 1 | \$730.22 | \$730.22 | https://thorlabs.com | Other |
| PA 2200* | 1,379.57 cm ³ | \$0.09/cc | \$124.16 | https://eos.info | Powder |

*Note that PA 2200 was printed in-house, and the costs provided reflect the rates charged by the AddFab facilities for the material and their services.

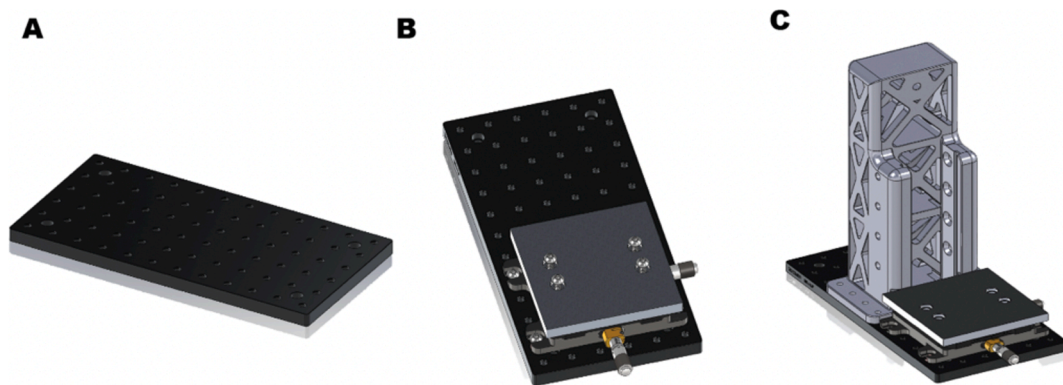


Fig. 2. CAD models for Base component (A) Base with motion plate, (B) Fixture plate with attached motion plate to, and (C) Fixture plate with attached motion plate and arm base.

6. Build Instructions

Construction requires screw drivers and wrenches of various sizes. Ensure you have the correct part sizes and tools to prevent potential challenges and enable smooth, efficient device assembly.

Printing Information

The parts were printed using the selective laser sintering (SLS) process on an EOS P110 machine. The material is BASF PA11 powder, printed with a bed temperature of 185C. Parts were depowdered, blasted with crushed glass abrasive, and water rinsed. The process is similar to that of commercial 3D printing service bureaus who use nylon-11 in an SLS process.

6.1. Base

Using a screwdriver, attach the motion stage to the fixture plate with four $\frac{1}{4}$ in-20 x $\frac{1}{4}$ in screws and screw in four $\frac{1}{4}$ in-20 x 5/8 in screws. Attach two shelves to the motion stage using four $\frac{1}{4}$ in-20 x 5/8 in screws as shown below (Fig. 2A-B). Fasten the arm base to the fixture plate using eight $\frac{1}{4}$ in-20 x 5/8 in screws (Fig. 2C).

6.2. Arm

***Safety tip:** It is recommended to wear cut resistant gloves when handling the sharp blade during assembly and operation

- 5.2.1. Push two bearings into the wheel (Fig. 3A-B).
- 5.2.2. Push two bearings into the lever (Fig. 3C).
- 5.2.3. Align the lever with the crank and screw three M2.5 x 14 mm screws through both (Fig. 3D-E).
- 5.2.4. Screw an M8x 30 mm screw through the wheel, an M8 nut and the larger side of the lever. (Fig. 3F).
- 5.2.5 Align the razor's holes with the three small holes on the razor holder and align the razor cover with the three-square slots (Fig. 3G-H).
- 5.2.6 Fasten the razor to the razor holder and razor cover using two M2.5 x .45 x 14 mm screws and two M2.5 nuts on the outer holes (Fig. 3I).
- 5.2.7 Place four M8 x 1.25 x 30 mm screws through four bearings and slide each of these into the front of the razor holder (Fig. 3J).
- 5.2.8. Put an M8 x 1.25 x 30 mm screw through the smaller side of the lever and then through the top of the razor holder (Fig. 3 K-L).
- 5.2.9. Slide the razor holder into the arm base slots.
- 5.2.10. Screw the M8 x 1.25 x 130 mm screw into the arm base so the end is just aligned with the wheel bearing outside face.

6.3. Box

Cut out the schematic of the box using a laser cutter and $\frac{1}{4}$ ” acrylic. Assemble the acrylic box and shell by connecting the slotted pieces, as illustrated in Fig. 4. To bond the box together, apply polydimethylsiloxane (PDMS, Sylgard 184 10:1 (w/w) base: curing agent) to the slotted components and cure in a 65 °C oven overnight.

7. Operation Instructions

Safety Tip: It is recommended to wear cut-resistant gloves when handling the sharp blade during assembly and operation.

Specimen preparation:

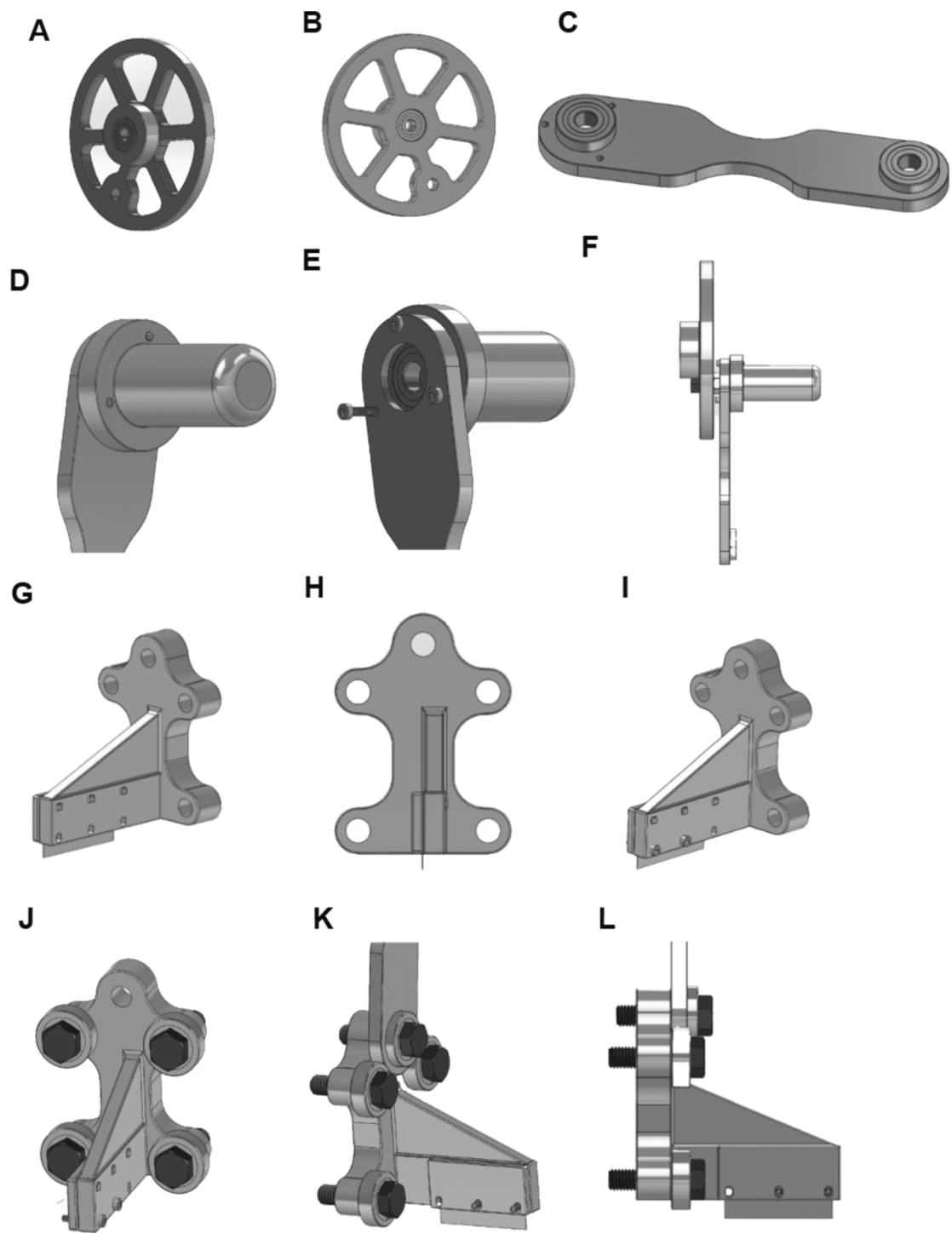


Fig. 3. CAD models for arm components. (A-B) Wheel with bearings; (C) Lever with bearings; (D-E) Lever with crank; (F) Lever and crank attached to wheel; (G-I) Razor holder and fastener with razor; (J) Razor holder with screws and bearings; (K-L) Razor holder attached to lever.

1. **Assemble the slicer components:** First, assemble the shell and box.
2. **Prepare the specimen:** Add a 1–2 mL layer of agarose into the box, followed by placing the organoids inside. Fill the rest of the box with additional agarose.

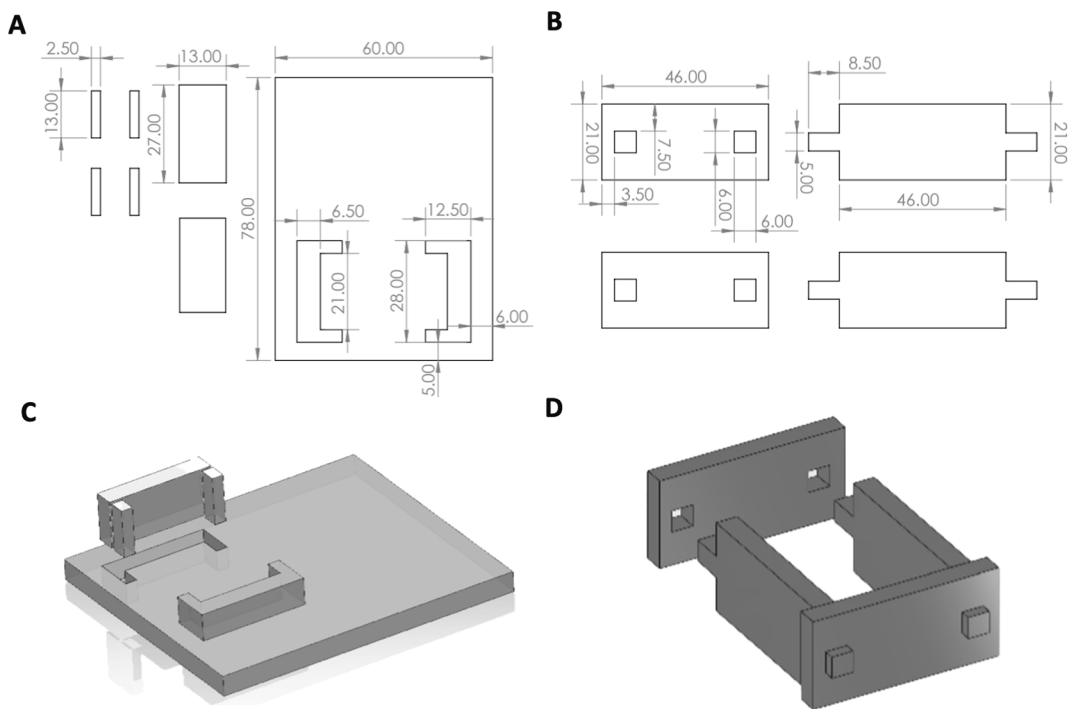


Fig. 4. Acrylic box and box shell (A) Schematic of acrylic box (B) Schematic of acrylic box shell (C) Box (D) Acrylic box shell.

3. **Solidify the agarose:** Place the box on ice to allow the agarose to solidify. Once the agarose is solid, remove the shell. No adhesives like superglue are needed, as the solidified agarose and box structure will securely hold the organoids in place. The box is positioned by sliding it into the shelves.
4. **Note on liquid usage:** Unlike traditional vibratomes, the specimen does not need to be submerged in liquid during slicing. Additionally, there is no need to collect each slice immediately, as the slices remain embedded within the agarose block, allowing multiple slices to be produced in succession. Given that only a few slices are typically obtained at a time, it is not necessary to keep the specimen cold. Unlike vibratomes, which require extended time and continuous cooling due to the large number of sections produced, our device slices within 5–10 min. The agarose is prepared with culture media, ensuring the tissue remains viable throughout the process without the need for cooling or submersion in media. However, after each slice is released from the agarose, it should be placed in DPBS to maintain viability.

Step-by-step slicing procedure:

1. Ensure the specimen is loaded into the box and stable.
2. Raise and stabilize the cutter before proceeding:
 - a. Use the crank handle to rotate the main wheel, lifting the razor to its highest point.
 - b. Insert the support screw through one of the top holes in the slotted supports.
 - c. Gently allow the cart to rest on the support screw, then release the system.
3. Slide the box under the shelves, ensuring it is oriented as shown in [Fig. 1](#).
4. Use the crank handle to raise the razor to its highest point, then hold it there while removing the support screw.
5. Lower the razor until it just touches the top of the specimen (without cutting it), and use the motion stage knob to align the razor with the desired cutting location.
6. Raise the razor back to its highest point with the crank handle, then rotate it one full loop to slice the specimen.
7. After completing a full loop, stabilize the cutter by inserting the support screw to hold the razor above the specimen.
8. Adjust the motion stage knob to set the thickness of the next cut.
9. Lift the razor, remove the support screw, and make another full loop to slice again.
10. After slicing is complete, stabilize the cutter, then gently slide the box out from the shelves to extract your specimen.

Settings for determining thickness:

The motion stage is measured in inches and can move a total of 0.5 in. in the x and y direction. One full rotation on the x knob is equivalent to 1/40 of an inch. Example: If you're desired slice thickness is 1.2 mm then the knob needs to be turned twice in the x direction.

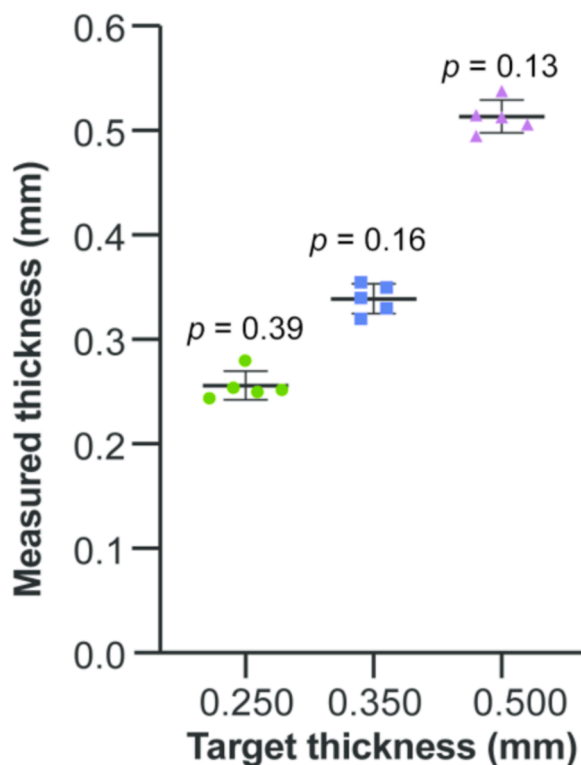


Fig. 5. The precision of slice thickness. Dot plots shown targeted thickness and actual slice thickness ($n = 5$ for each thickness). Error bars indicate standard error of mean, and p values are calculated using one-sample student t -test.

Settings for rotational speed:

It is recommended to operate the slicer at 1 rotation/5 s. Our characterization of the precision and straightness of the slicing was done at 1 rotation/5 s. Operating at this speed ensured that the slices were both straight and precisely cut the desired thickness each time it was operated. A quick experiment, operating the slicer at 1 rotation/1 s lead to less precise cuts where the target thickness being 0.75 mm and the slice resulted in 0.55 mm. Users should use the recommend settings to minimize variability.

8. Validation and characterization

A relevant use case for this particular hardware would be slicing a centre piece out of an agarose embedded live brain organoid with precision and accuracy. In typical organoids culture, significant necrosis and non-functional cells are often found in the core of organoids due to the diffusion limit of oxygen and nutrients. Recent studies have demonstrated that sliced brain organoids show improved cell viability and functional activities [4]. Therefore, here we will use slicing brain organoids as an example to characterize the performance of our device in terms of slicing precision, cut straightness, and cell viability after slicing.

8.1. Precision of the slice thickness

We first tested the precision of the slice thickness by comparing the actual slice thickness with targeted thickness. Agarose gel block was sectioned at three distinct target thicknesses (0.250 mm, 0.350 mm, and 0.500 mm, respectively), which were typically used in slicing organoids considering diffusion limits. Slices aimed at a thickness of 0.250 mm, averaged a measurement of 0.256 ± 0.006 mm. 0.350 mm slices yielded an average thickness of 0.339 ± 0.006 mm. For 0.500 mm slices, the average thickness was determined to be 0.513 ± 0.007 mm. No statistical significance between the targeted value and the slices sectioned were found for all three thicknesses (Fig. 5).

8.2. Cut straightness Testing

We measured cut straightness through the agarose by characterizing the z-axis deflection. We took a macro shot video of the acrylic box with agarose stabilized. By imaging analysis, we were able to model scaled axes (in mm) to the macro shot video and measure the deflection from a vertical line from the base. We then noted the z-axis deflection at 1, 2, 3, 4 and 5 mm above the box base by pausing the video at each mm above the box base. We found an average z-axis deflection of $\Delta z = 0.115 \pm 0.015$ mm and no statistical

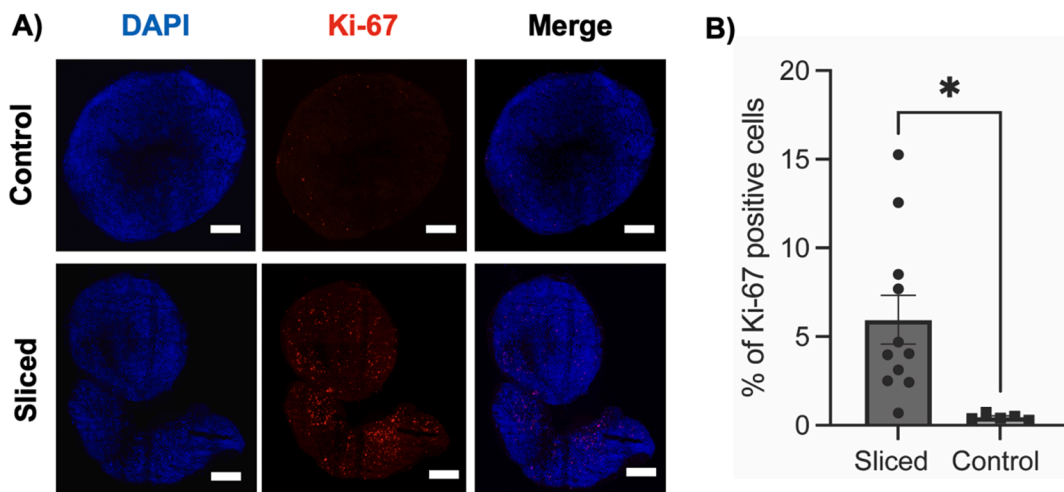


Fig. 6. Immunostaining of sliced organoids showing improved cell proliferation. A) Representative confocal microscopy images showing DAPI staining (blue) indicating cell nuclei and red fluorescence indicating Ki-67 positive cells in sliced and control organoids. B) Bar plot quantification of Ki-67 positive cells. Error bars indicate standard error of mean, and p values are calculated using two-sample student t -test. Scale bar, $\sim 200\mu\text{m}$. *, $p < 0.05$. (For interpretation of the references to colour in this figure legend, the reader is referred to the web version of this article.)

significance was found when compared to perfectly straight slice, or $\Delta z = 0$, ($p = 0.070$, one-sample student t -test).

8.3. Organoid viability tests

To assess the viability of organoids post-slicing, we quantified the ratio of proliferating cells to total cells. Brain organoids were derived from human embryonic stem cells using a previously published protocol (6). Organoid slicing was conducted on day 153 of organoid maturation, followed by a five-day post-slicing culture period. Subsequently, the slices were fixed and stained with Ki-67 antibody to visualize cell proliferation, alongside DAPI staining. Quantification of Ki-67 and DAPI signals using Nikon Elements –GA3 software revealed a significantly higher percentage of Ki-67 + cells in sliced organoids compared to the unsliced controls (Fig. 6). This suggests that sliced organoids are actively proliferating, indicating that slicing does not compromise their viability, and improved nutrient and oxygen diffusion facilitate the development of organoids.

9. Discussion

Organoids that were not sliced exhibited sparse Ki67 detection, whereas those that were sliced showed an abundance of Ki67-positive cells. In our study, organoids sliced at day 153 exhibited Ki67 positivity in 5–15 % of the total cell population, compared to less than 3 % in control unsliced organoids. A previous study using a Leica vibratome to slice organoids at day 150 reported similar trends, with an abundance of Ki67-positive cells in the progenitor zones at approximately 15 %, while unsliced organoids showed sparse Ki67 presence in the progenitor zones, around 5 % [5]. While that study focused specifically on progenitor zones and ours on the entire organoid, the overall values and trends are comparable. The large variability between the sliced and control organoids is expected due to intrinsic heterogeneity of neural organoids and random distribution of proliferating neural progenitor cells [6].

While our low-cost slicer has been shown to effectively section brain organoids in hydrogels with minimal impact on cell viability, there are some limitations when translating this technology to other tissue types, such as brain, tumor, or lymph node explants. For softer tissues, like actual brain tissue, the absence of vibration in our slicer could lead to less precise cuts and increased tissue damage, as these tissues are more delicate compared to the agarose gel used in our experiments. Additionally, our system requires tissue embedding in agarose, which may compromise cell viability in certain tissues, particularly if longer slicing times are needed. However, in cases where gel embedding is feasible and only a few slices are required, our slicer could still provide a useful, low-cost alternative for tissue sectioning.

While this alternative is cost-effective, it does have certain limitations. Unlike vibratomes, the organoids are not immersed in a buffer or maintained in a O_2 -enriched environment, requiring slices to be made quickly to preserve viability. Additionally, the manual cranking mechanism introduces variability in the applied force, potentially leading to inconsistent results across users. To address these limitations, automation of the device would be a beneficial improvement. Integrating an image recognition system to detect the organoid and automatically control the stage for precise slicing could standardize results and enhance reproducibility. Furthermore, enlarging the sample chamber to accommodate a buffer and O_2 , as is done with vibratomes, would improve organoid viability over longer periods.

Declaration of Generative AI and AI-assisted technologies in the writing process

During the preparation of this work the author(s) used ChatGPT in order to correct for grammar and punctuation. After using this

tool/service, the author(s) reviewed and edited the content as needed and take(s) full responsibility for the content of the publication.

CRediT authorship contribution statement

Beatriz Martinez-Martin: Writing – original draft, Validation, Formal analysis, Data curation, Conceptualization. **Isabella Lambros:** Writing – original draft, Methodology, Data curation, Conceptualization. **Lukas Nuesslein:** Data curation. **Yubing Sun:** Writing – review & editing, Supervision, Conceptualization.

Declaration of competing interest

The authors declare that they have no known competing financial interests or personal relationships that could have appeared to influence the work reported in this paper.

Acknowledgments

This work was supported by the National Institute of Mental Health (R21MH130843 to Y.S.) and the National Science Foundation (CMMI-1846866 and CBET-2326703 to Y.S. and REU supplements to I.L.). This work was supported in part by a Fellowship from the University of Massachusetts to B. M. as part of the Biotechnology Training Program (National Research Service Award T32GM135096). Additionally, the authors would like to thank David Follette the Advanced Digital Design and Fabrication (ADDFab) Director and ADDFab personnel for their support in 3D printing parts.

Appendix A. Supplementary data

Supplementary data to this article can be found online at <https://doi.org/10.1016/j.ohx.2024.e00611>.

References

- [1] G. T. Prusky, J. E. McKenna, Serial sectioning of thick tissue with a novel vibrating blade microtome, *Brain Res. Protoc.* 3 (1999) 302-307. [https://doi.org/10.1016/s1385-299x\(98\)00052-x](https://doi.org/10.1016/s1385-299x(98)00052-x).
- [2] F. Siwczak, C. Hiller, H. Pfannkuche, M.R. Schneider, Culture of vibrating microtome tissue slices as a 3D model in biomedical research, *J. Biol. Eng.* 17 (2023), <https://doi.org/10.1186/s13036-023-00357-5>.
- [3] M. Diem, M. Romeo, S. Boydston-White, M. Miljkovic, C. Matthäus, A decade of vibrational micro-spectroscopy of human cells and tissue (1994-2004), *Analyst* 129 (2004) 880-885. <https://doi.org/10.1039/b408952a>.
- [4] X. Qian, et al., Sliced human cortical organoids for modeling distinct cortical layer formation, *Cell Stem Cell* 26 (2020) 766-781.e769 <https://doi.org/10.1016/j.stem.2020.02.002>.
- [5] T. Sharf, et al., Functional neuronal circuitry and oscillatory dynamics in human brain organoids, *Nat. Commun.* 13 (2022) 4403, <https://doi.org/10.1038/s41467-022-32115-4>.
- [6] O.L. Eichmüller, J.A. Knoblich, Human cerebral organoids — a new tool for clinical neurology research, *Nat. Rev. Neurol.* 18 (2022) 661–680, <https://doi.org/10.1038/s41582-022-00723-9>.



Beatriz Martinez-Martin is a third-year PhD candidate in the Molecular and Cellular Biology program at the University of Massachusetts Amherst. She is currently conducting research as a joint student in the labs of Dr. Yubing Sun and Dr. ChangHui Pak, focusing on the development of technologies to enhance brain organoid models. Beatriz earned her Bachelor of Arts in Biology from the University of San Diego, where she conducted research in Dr. Nicole Danos' lab. She is an active member of the Society for the Advancement of Chicanos/Hispanics, the International Society for Stem Cell Research, and the Biomedical Engineering Society.



Isabella Lambros holds a Bachelor of Applied Science in Mechanical Engineering from the University of Massachusetts Amherst. She is specialized in CAD and FEA and has used her specialty to work on a variety of projects including an award winning Floating Wind Challenge. She is currently pursuing a career in Renewable energy but has ample amounts of experience in biomedical engineering.



Lukas Nuesslein is a junior undergraduate pursuing a Bachelor of Science in Mechanical Engineering at the University of Massachusetts Amherst. He specializes in CAD and is an active member of the UMass Aeronautics Team where he uses his knowledge in depth to help design and manufacture a remote-controlled airplane for a national competition. He has experience working in the Crosby Research Group at UMass Amherst where he researched polymers and their tensile strength. He is currently working in the lab of Dr. Yubing Sun, where he is assisting with organoid research, mainly designing and manufacturing parts for organoid culture.



Yubing Sun is an Associate Professor in the Department of Mechanical and Industrial Engineering at the University of Massachusetts Amherst. He received his Ph.D. degree from the Department of Mechanical Engineering at the University of Michigan, Ann Arbor in 2015, and his B.S. degree in Materials Science and Engineering from the University of Science and Technology of China. Dr. Sun has been recognized by NIGMS MIRA Award, NSF CAREER Award and Barbara H. and Joseph J. Goldstein Outstanding Junior Faculty Award at UMass. His current research interests include stem cell biology, organoid engineering, microfabrication, developmental biomechanics, lab-on-chip, and bio-sensing. He is an Associate Editor of *Frontier in Bioengineering and Biotechnology*, editor board member of *Scientific Reports*, *Molecular & Cellular Biomechanics*, and *Micromachines*.